

Communication

Recent Results from LUX and Prospects for Dark Matter Searches with LZ[†]

Vitaly A. Kudryavtsev for the LUX and LZ Collaborations

Department of Physics and Astronomy, University of Sheffield, Sheffield S3 7RH, UK;
v.kudryavtsev@sheffield.ac.uk

[†] This paper is based on the talk at the 7th International Conference on New Frontiers in Physics (ICNFP 2018), Crete, Greece, 4–12 July 2018.

Received: 17 January 2019; Accepted: 1 March 2019; Published: 7 March 2019



Abstract: Weakly Interacting Massive Particle (WIMP) remains one of the most promising dark matter candidates. Many experiments around the world are searching for WIMPs and the best current sensitivity to WIMP-nucleon spin-independent cross-section is about 10^{-10} pb. LUX has been one of the world-leading experiments in the search for dark matter WIMPs. Results from the LUX experiment on WIMP searches for different WIMP masses are summarised in this paper. The LUX detector will be replaced by its successor, the LUX-ZEPLIN (LZ) detector. With 50 times larger fiducial mass and an increased background rejection power due to specially-designed veto systems, the LZ experiment (due to take first data in 2020) will achieve a sensitivity to WIMPs exceeding the current best limits by more than an order of magnitude (for spin-independent interactions and for WIMP masses exceeding a few GeV). An overview of the LZ experiment is presented and LZ sensitivity is discussed based on the accurately modelled background and the high-sensitivity material screening campaign.

Keywords: dark matter; WIMPs; radioactivity; detectors; underground experiments

1. Introduction

Astrophysical and cosmological observations favour the Λ CDM model of the structure and evolution of the Universe that includes, as main constituents, baryonic matter, dark matter and dark energy. Precision cosmology determines the fraction of each component to within a few percent or better, with about a quarter of matter-energy density being associated with non-baryonic dark matter. One of the most promising dark matter candidates is the Weakly Interacting Massive Particle (WIMP) that is characterised by a high mass (typically within the 1–1000 GeV/ c^2 range) and a small interaction cross-section (at a weak scale). A good candidate is provided by Supersymmetry (i.e., the lightest supersymmetric particle or neutralino).

A number of experiments around the world are searching for WIMPs, among which those using the dual-phase xenon technique, such as LUX [1], and then Panda-X [2] and XENON1T [3], have achieved the best sensitivity to date for WIMPs with masses exceeding a few GeV. The LUX-ZEPLIN (LZ) experiment [4] will be leading the search for dark matter particles from 2020.

2. WIMP Detection with Dual-Phase Xenon Detectors and the LUX Experiment

The LUX detector exploits the excellent properties of the Time Projection Chamber (TPC) with liquid xenon (LXe) as a target, to search for WIMP interactions within a large background from radioactivity and spurious events. The principle of particle detection in a dual-phase xenon TPC is illustrated in Figure 1 (left) [5]. LXe serves as the main target for particle interactions. LXe, known to be a good scintillator, produces scintillation light (S1 signal) when a particle deposits energy within

the target. The light is detected by two arrays of photomultiplier tubes (PMTs) on the top and bottom of the detector (mainly in the bottom array due to reflection from the liquid/gas interface). Particle interaction also causes ionisation of atoms in LXe, whereas an applied electric field suppresses electron-ion recombination and allows electrons to drift upwards, towards the gas phase. Electrons are then extracted from the liquid into the gas and produce the delayed signal (S2) by electroluminescence that is seen by the PMTs (mainly in the top array). The pattern of light in the top PMT array from S2 provides the $x - y$ coordinates (in the horizontal plane) of the original energy deposition with an accuracy of about 1 cm for low-energy events, whereas the time delay between S1 and S2 determines the position along the vertical z -axis with a few mm accuracy [6]. In addition, the ratio of S2/S1 provides a very good discrimination power between the nuclear recoils (NRs) expected from WIMP interactions (also from the neutron background) and electron recoils (ERs) from the main background of gamma-rays and beta-decays. Figure 1 (right) shows the inner part of the LUX TPC, without the bottom PMT array. A detailed description of the LUX experiment including early calibrations, event reconstruction, and data analysis procedures, have been reported in [7]. The total active xenon mass (within the TPC) was 250 kg, with the inner fiducial volume for WIMP searches containing about 100 kg of xenon. The search for WIMP interactions involved identifying single-hit NR events, potentially caused by WIMPs, in a background of ERs, based on the S2/S1 ratio that was measured to be significantly smaller for NRs than for ERs for a fixed, measured S1 signal [7]. Only single-hit events were considered as candidates for dark matter particle interactions, whereas multiple hit events were associated with the background.

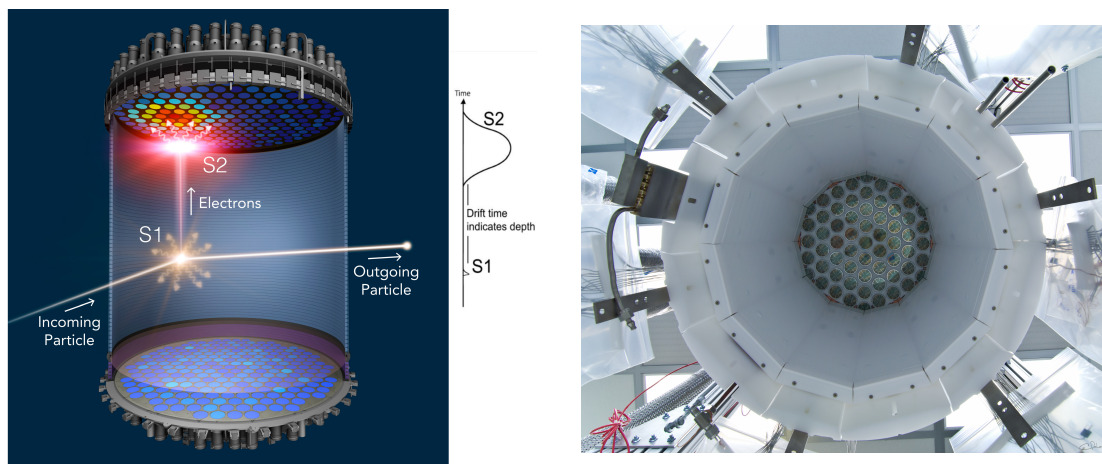


Figure 1. (Left) The operating principle of the dual-phase xenon TPC. An electric field is applied along the cylindrical part of the TPC, allowing electrons to drift towards the anode. Each particle interaction in the active LXe produces two signals: the first one comes from the prompt scintillation (S1) and the second one, delayed by the electron drift time, comes from ionisation, by electroluminescence in the gas phase (S2). See text for detail. (Right) Photo of the inner part of the LUX TPC, without the bottom PMT array.

The LUX detector was immersed in a large water tank that provided shielding against gamma-rays and neutrons from the surrounding rock. Cosmic-ray muon flux was attenuated by about 6 orders of magnitude by rock above the detector, being located at a depth of about 1480 m below ground in the Sanford Underground Research Facility (SURF) (Lead, SD, USA).

After 3.35×10^4 kg·days of running the experiment, no statistically significant excess of single-hit events in the fiducial volume over the background-only model was found that resulted in the limit on the spin-independent WIMP-nucleon cross-section of 1.1×10^{-46} cm² at the minimum of the sensitivity curve (about 50 GeV/c²) [1]. These limits were world-leading at the time of the experiment.

The same data, interpreted as WIMP-proton/neutron spin-dependent interactions, results in limits on spin-dependent cross-sections [8].

In addition to ‘standard’ WIMPs, the search for axions and axion-like particles (ALPs) in the collected data has been performed. As axions and ALPs interact through the axioelectric effect (similar to photoelectric effect), their interactions would produce single-hit ERs that would have an S_2/S_1 ratio similar to that measured for background ERs, making this search more challenging and largely dependent on the background event rate. The low background conditions of the LUX experiment and the absence of an excess of ERs over the rate predicted by a background model, allowed us to set strict limits on the axion-electron coupling constant, reported in [9].

An important result of the LUX experiment is the measurement of the total rate of events at low energies (without rejecting electron recoil events) and the amplitude of a potentially modulated signal. This measurement provided an unambiguous rejection of the claim from the DAMA experiment about their observation of the annual modulation of the dark matter signal. LUX measured the total single-hit event rate in the fiducial volume (signals of all types are included: electron and nuclear recoils) to be about 2×10^{-3} events/kg/day/keV at 2–6 keV [10], compared to the average amplitude of modulation of about 10^{-2} events/kg/day/keV at 2–6 keV, reported by DAMA/LIBRA [11]. The total single-hit rate in the LUX fiducial volume at 2–6 keV was about 500 times lower than in DAMA (5 times smaller than the amplitude of modulation). No statistically significant annual or diurnal modulation was observed by the LUX experiment, the former being, again, in direct confrontation with the DAMA measurements that showed a 12.9σ effect of the annual modulation [11].

Ultra-low background conditions in the fiducial volume of LUX allow us to extend searches below traditional WIMP mass range, moving towards low masses. An interesting possibility is offered by models where standard NRs from WIMP-nucleon interactions are accompanied by electron emission from atoms, due to bremsstrahlung [12] or Migdal [13] effects. For low-mass WIMPs, the NR signal could be below the detector energy threshold (due to quenching of scintillations from NRs), but the signal from ERs may be detectable. LUX data, collected in 2013, have been analysed to search for any possible excess of ER events at low energies. Figure 2 (left) shows the regions where the ERs from the WIMP-nucleon interactions, and where bremsstrahlung and Migdal effects are expected for different WIMP masses, superimposed on the LUX data. The limits on WIMP-nucleon cross-section extracted from LUX data are shown in Figure 2 (right). The contours on the left panel are overlaid on 591 events, observed in the region of interest from the 2013 LUX exposure of 95 live days and 145 kg fiducial mass [14]. Points at radius <18 cm within the TPC are black; those at 18–20 cm are grey, and these are more likely to be caused by radio-contaminants giving signals near the detector walls. Bands of electron recoil events uniform in energy (blue) and an example of NR signals from 150 GeV/ c^2 WIMPs (red) are indicated by 50th (solid), 10th, and 90th (dashed) percentiles of S_2 at given S_1 . Grey lines, showing the ER energy scale of keVee at the top and the NR energy scale of keVnr, from the Lindhard model, at the bottom, are contours of the combined S_1/S_2 energy estimator. Figure 2 (right) shows the WIMP-nucleon cross section limits at 90% C.L., as calculated using the bremsstrahlung and Migdal effect signal models assuming a scalar mediator (coupling proportional to A^2).

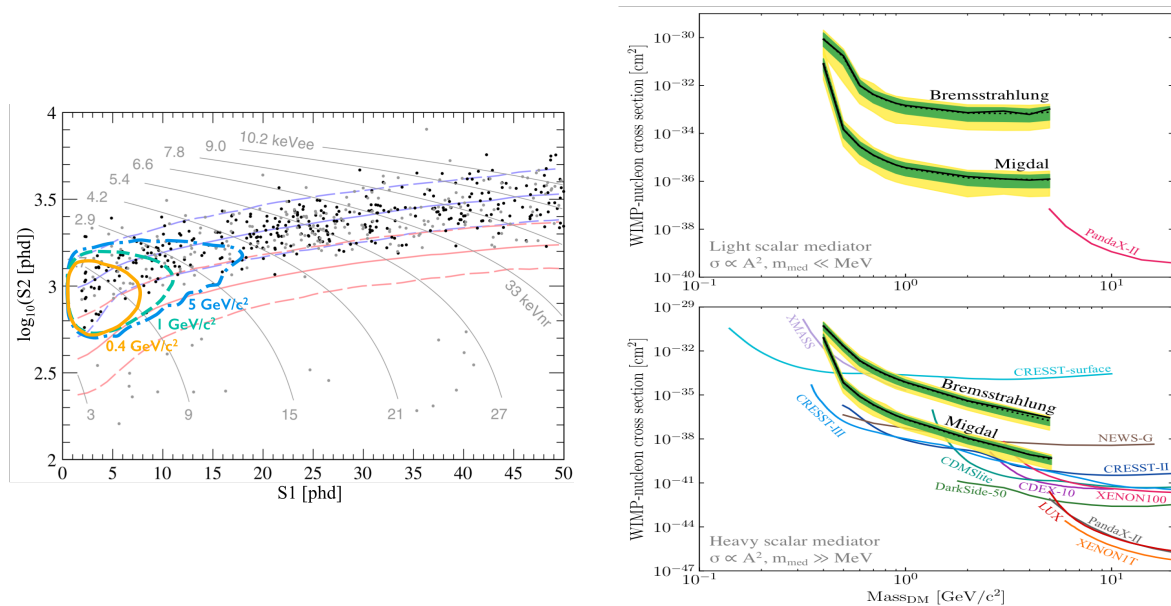


Figure 2. (Left) Contours containing 95% of the expected WIMP signal from the bremsstrahlung and Migdal effects. Different contours indicate expected signal in different models: bremsstrahlung signal from $0.4 \text{ GeV}/c^2$ WIMPs assuming a heavy scalar mediator, Migdal effect from $1 \text{ GeV}/c^2$ WIMPs assuming a heavy scalar mediator, and Migdal effect from $5 \text{ GeV}/c^2$ WIMPs assuming a light vector mediator (see text for detail). (Right) WIMP-nucleon cross section limits at 90% C.L., as calculated using the bremsstrahlung and Migdal effect signal models assuming a scalar mediator (coupling proportional to A^2). The 1σ and 2σ ranges of background-only trials for this result are shown as green and yellow bands, respectively, with the median limit shown as a black curve. The top figure presents the limit for a light mediator with the reference value for the 4-momentum transfer in the form-factor $q_{\text{ref}} = 1 \text{ MeV}$. The bottom figure shows limits for a heavy mediator, along with limits from the standard NR analyses of other experiments [14].

3. The LZ Experiment

The LZ detector is the next-stage direct dark matter search experiment, with improved sensitivity to WIMPs. The principle of operation is the same one as used in its predecessor—LUX. LZ will contain 10 tonnes of liquid xenon, with 7 tonnes of xenon being an active mass inside the TPC. The active volume will be viewed by 494 PMTs, positioned on the top and bottom of the cylindrical TPC. The rejection of the background signal is improved, compared to LUX, by adding a LXe ‘skin’ region outside the TPC, viewed by a set of additional PMTs. Also, an additional outer detector (OD), made of liquid organic scintillator loaded with Gd salt to enhance neutron capture, will be installed around the cryostat with LXe. The purpose of the skin and the liquid scintillator is to tag background gamma-rays (mainly in the xenon skin) and neutrons (mainly in the Gd-loaded scintillator). All detector systems will be immersed in a water tank (same as in the LUX experiment). Outer detector PMTs will be positioned on a cylindrical support structure inside the water, and will collect the light from the liquid scintillator and water, thus detecting signals from the captured neutrons and events associated with cosmic-ray muons. The schematic diagrams of the LZ detector are shown in Figure 3 [4].

The principle of LZ operation is similar to that of LUX. Primary scintillation (S1) and secondary ionisation (S2, by electroluminescence) signals will be detected by the arrays of PMTs on the top and bottom of the TPC. The S2 signal is caused by electrons drifting upwards in an electric field and extracted into the Xe gas. Position sensitivity is achieved by measuring the drift time (proportional to the distance from the gas phase) and the pattern of light from the S2 signal in the top PMT array. Multiple hit events and coincidences with the xenon skin or the OD (within $500 \mu\text{s}$) will be rejected as being caused by the background. The inner fiducial volume containing 5.6 t of LXe, is defined based

on simulations to remove ERs and NRs coming from the walls, PMTs, and grids. Further suppression of the ERs will be achieved by considering the S2/S1 ratio measured to be significantly lower for NRs than for ERs.

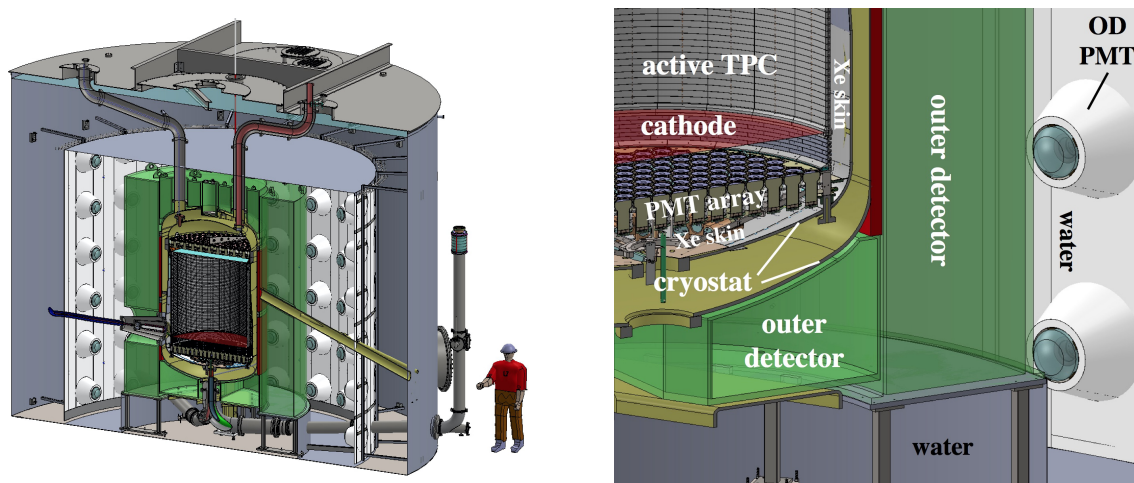


Figure 3. (Left) Schematic diagram of the LUX-ZEPLIN (LZ) detector. The LXe TPC is surrounded by the outer detector tanks (green) and light collection system (white), all housed in a large water tank (blue-grey). Conduits deliver services to various detector systems: PMT and instrumentation cables (top and bottom, red); cathode high voltage (lower left with cone); purified LXe (bottom centre, green); neutron beam conduit (right, yellow). (Right) Expanded view of the lower right corner. The xenon skin region is viewed by a separate set of PMTs (not visible here).

Continuous online purification of xenon will lead to a reduction of ^{222}Rn contamination (due to radon emanation from materials and dust particulates inside the cryostat), down to about $1.8 \mu\text{Bq/kg}$, and to a high lifetime of drifting electrons (exceeding the maximum drift time of $800 \mu\text{s}$). Natural Kr will be reduced to a level of 0.015 ppt of xenon.

LZ will deploy a number of calibration systems to define the S1 and S2 energy scales, ER and NR bands on the S2/S1 versus S1 plot to search for WIMP-induced events, to quantify the accuracy of position reconstruction, and to calibrate the xenon skin and the OD. Calibration sources will include radioactive materials, such as dispersed isotopes of $^{131\text{m}}\text{Xe}$, $^{83\text{m}}\text{Kr}$, ^{220}Rn and tritium (tritiated methane), an external gamma-ray source ^{22}Na , external neutron sources (AmLi, AmBe, and ^{88}YBe), and a DD neutron generator.

An intensive material screening campaign is being carried out to identify radioactive contaminants and select materials for detector components that satisfy radio-purity requirements. Measured radioactivities are used to normalise simulations of backgrounds carried out with the specially developed Monte Carlo code BACCARAT based on the GEANT4 toolkit. Figure 4 shows simulated energy spectra of ERs, as expected from various sources. The background in the energy range of interest in the LZ fiducial volume is dominated by the internal xenon contaminants, in particular ^{222}Rn , and the physics background, especially from solar neutrinos. A detailed analysis can be found in [4]. Assuming, conservatively, 99.5% ER rejection using the S2/S1 ratio and 50% NR signal acceptance, the total background after all cuts is calculated as about 6.5 events in 1000 days, in a 5.6 tonne fiducial mass. This includes events in the 1.5–6.5 keV range for electron recoils and the 6–30 keV range for nuclear recoils; typical for about $40 \text{ GeV}/c^2$ WIMPs. This also excludes events from solar neutrinos that will lie outside the nuclear recoil band defined for $40 \text{ GeV}/c^2$ WIMPs.

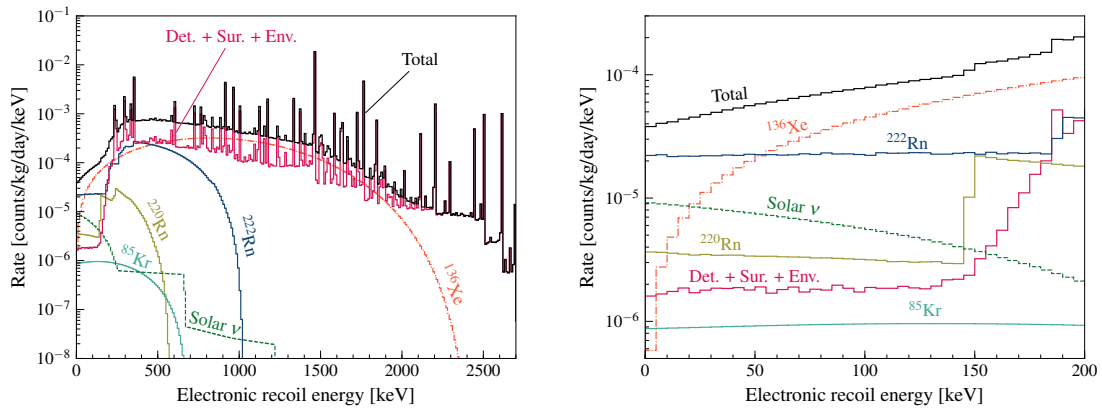


Figure 4. (Left) Simulated background spectra of electron recoils (ERs) in the 5.6 tonne fiducial volume for single-hit events not accompanied by any signal in the xenon skin or the outer detector. No detector efficiency, detector response, or WIMP-search region of interest cuts on S1 have been applied. (Right) Similar ER spectra as in the left panel, but for the 0–200 keV energy range.

Figure 5 shows a simulated distribution of nuclear recoils in the active volume of the TPC (NRs from solar neutrinos or wall events caused by NRs exiting the surfaces of the TPC are not included). A significant reduction in the NR background (by about a factor of 10) is achieved using the veto systems.

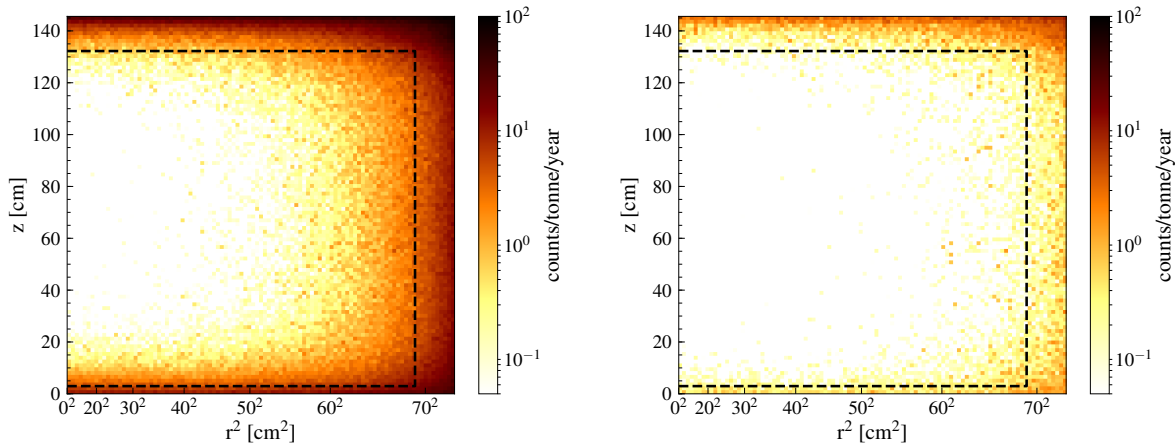


Figure 5. (Left) Positions of single hit NR events in the region of interest relevant to a 40 GeV/c² WIMP (approximately 6–30 keV) with no vetoing. The total count for the 5.6 tonne fiducial volume (dashed line) is 10.43 events/1000 days. (Right) Similar scatter plot, but after rejecting events in coincidence with the xenon skin (above 100 keV threshold within the time window of 800 μs limited by the maximum drift time) and the outer detector (above 200 keV threshold within the time window of 500 μs). The total background from NRs is now reduced to 1.03 events/1000 days [4].

Figure 6 shows an example scatter plot of S2 versus S1 for simulated background events in 1000 days and for a 5.6 tonne fiducial mass, after all cuts were applied. An ER band with higher values of S2 is populated by background events from radioactive contaminants inside the LXe (e.g., ²²²Rn), radioactivity in materials, and environment and physics backgrounds (two-neutrino double-beta decay and solar neutrinos). NRs from solar neutrinos appear in a region with low S1 and low S2.

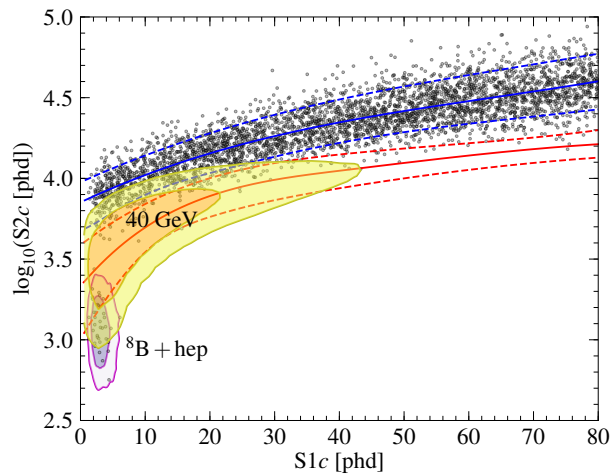


Figure 6. Scatter plot of an example data set of simulated events from background in 1000 live days and a 5.6 tonne fiducial mass. ER and NR bands are indicated in blue and red, respectively (solid: mean value; dashed: areas for 10% and 90% populations). The 1σ and 2σ contours for low-energy NRs from ^8B and hep solar neutrinos, and a $40 \text{ GeV}/c^2$ WIMP are shown as shaded regions [4].

Figure 7 shows the projected sensitivity of the LZ experiment after 1000 days of live time. The left panel presents the exclusion limits, whereas the right panel shows the discovery potential. The analysis of the profile likelihood ratio is used for the plots. The best exclusion sensitivity of $1.6 \times 10^{-48} \text{ cm}^2$ is achieved at a WIMP mass of $40 \text{ GeV}/c^2$. The best $3(5)\sigma$ significance for a WIMP discovery is achieved at $3.8(6.7) \times 10^{-48} \text{ cm}^2$ for $40 \text{ GeV}/c^2$ WIMPs.

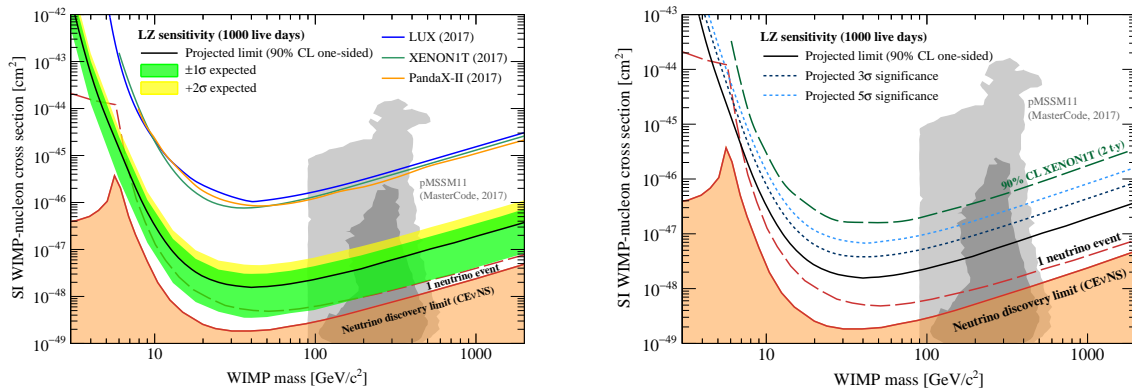


Figure 7. (Left) LZ projected sensitivity to spin-independent WIMP-nucleon elastic scattering for 1000 live days and a 5.6 tonne fiducial mass, together with the results from the other LXe experiments. The lower shaded region and dashed line indicate the limitations from the coherent scattering of neutrinos and the grey contoured regions show the favoured regions from recent pMSSM11 model scans (see [4] for a detailed description). (Right) LZ discovery potential for spin-independent WIMP-nucleon scattering. The projected sensitivity of a 2 t-y exposure of XENON1T [15] is shown for comparison.

4. Conclusions

Liquid xenon TPCs have shown to be the most powerful instruments in the search for WIMP dark matter. LUX has set the most stringent limits at the time of running, on various scenarios of WIMP interactions with the LXe target. The new LZ experiment, currently under construction, will extend the sensitivity to an unprecedented level, practically touching a ‘neutrino floor’—the background caused by solar and atmospheric neutrinos. With 7 tonnes of active mass of xenon, LZ will search for dark

matter WIMPs, neutrino-less double-beta decays, axions and ALPs, as well as for other phenomena predicted by theories beyond the Standard Model. LZ will begin its operations in 2020.

Funding: This work was supported by the U.S. Department of Energy (DOE) Office of Science under contract DE-AC02-05CH11231; by the U.S. National Science Foundation (NSF); by the U.K. Science & Technology Facilities Council under awards ST/M003655/1, ST/M003981/1, ST/M003744/1, ST/M003639/1, ST/M003604/1, and ST/M003469/1; by the Portuguese Foundation for Science and Technology (FCT) under awards CERN/FP/123610/2011 and PTDC/FISNUC/1525/2014; and by the Institute for Basic Science, Korea (budget numbers IBS-R016-D1 and IBS-R016-S1).

Acknowledgments: We acknowledge a huge support provided from the South Dakota Science and Technology Authority (SDSTA), which developed the Sanford Underground Research Facility (SURF) with an important philanthropic donation from T. Denny Sanford, as well as support from the State of South Dakota. SURF is operated by the SDSTA under contract to the Fermi National Accelerator Laboratory for the DOE, Office of Science. We would like to thank the Boulby Underground Laboratory (STFC) for continuous support of the LZ experiment through the screening of materials for radioactivity.

Conflicts of Interest: The authors declare no conflict of interest.

References

1. Akerib, D.S.; et al. [LUX Collaboration]. Results from a Search for Dark Matter in the Complete LUX Exposure. *Phys. Rev. Lett.* **2017**, *118*, 021303. [[CrossRef](#)] [[PubMed](#)]
2. Cui, X.; et al. [PandaX-II Collaboration]. Dark Matter Results from 54-Ton-Day Exposure of PandaX-II Experiment. *Phys. Rev. Lett.* **2017**, *119*, 181302. [[CrossRef](#)] [[PubMed](#)]
3. Aprile, E.; et al. [XENON Collaboration]. Dark Matter Search Results from a One Ton-Year Exposure of XENON1T. *Phys. Rev. Lett.* **2018**, *121*, 111302. [[CrossRef](#)] [[PubMed](#)]
4. Akerib, D.S.; et al. [LZ Collaboration]. Projected WIMP Sensitivity of the LUX-ZEPLIN (LZ) Dark Matter Experiment. *arXiv* **2018**, arXiv:1802.06039.
5. Mount, B.J.; et al. [LZ Collaboration]. The LUX-ZEPLIN (LZ) Technical Design Report. *arXiv* **2017**, arXiv:1703.09144v1.
6. Akerib, D.S.; et al. [LUX Collaboration]. Position Reconstruction in LUX. *J. Instrum.* **2018**, *13*, P02001. [[CrossRef](#)]
7. Akerib, D.S.; et al. [LUX Collaboration]. Calibration, Event Reconstruction, Data Analysis and Limits Calculation for the LUX Dark Matter Experiment. *Phys. Rev. D* **2018**, *97*, 102008. [[CrossRef](#)]
8. Akerib, D.S.; et al. [LUX Collaboration]. Limits on Spin-Dependent WIMP-Nucleon Cross Section Obtained from the Complete LUX Exposure. *Phys. Rev. Lett.* **2017**, *118*, 251302. [[CrossRef](#)] [[PubMed](#)]
9. Akerib, D.S.; et al. [LUX Collaboration]. First Searches for Axions and Axion-like Particles with the LUX Experiment. *Phys. Rev. Lett.* **2017**, *118*, 261301. [[CrossRef](#)] [[PubMed](#)]
10. Akerib, D.S.; et al. [LUX Collaboration]. Search for Annual and Diurnal Rate Modulations in the LUX Experiment. *Phys. Rev. D* **2018**, *98*, 062005. [[CrossRef](#)]
11. Bernabei, R.; Belli, P.; Bussolotti, A.; Cappella, F.; Caracciolo, V.; Cerulli, R.; Dai, C.-J.; D'Angelo, A.; Di Marco, A.; He, H.-L.; et al. First Model Independent Results from DAMA/LIBRA—Phase2. *Universe* **2018**, *4*, 116. [[CrossRef](#)]
12. Kouvaris, C.; Pradler, J. Probing Sub-GeV Dark Matter with Conventional Detectors. *Phys. Rev. Lett.* **2017**, *118*, 031803. [[CrossRef](#)] [[PubMed](#)]
13. Ibe, M.; Nakano, W.; Shoji, Y.; Suzuki, K. Migdal Effect in Dark Matter Direct Detection Experiments. *J. High Energy Phys.* **2018**, *3*, 194. [[CrossRef](#)]
14. Akerib, D.S.; et al. [LUX Collaboration]. Results of a Search for Sub-GeV Dark Matter Using 2013 LUX Data. *arXiv* **2018**, arXiv:1811.11241v1.
15. Aprile, E.; et al. [XENON Collaboration]. Physics Reach of the XENON1T Dark Matter Experiment. *JCAP* **2016**, *1604*, 027; arXiv:1512.07501.

